

CHARACTERIZATION OF FOAM BALLS LIGHTWEIGHT CONCRETE

Sohila A. El-Khouly, Randa Fouad, Amr H. Zaher, Ehab F. Sadek and Khalid M. Hilal

Abstract—An innovative and a new kind of lightweight concrete (LWC) was developed few years ago at the Department of Structural Engineering of Ain Shams University. It is called foam balls lightweight concrete (FBLWC), in which conventional aggregates are partially replaced by polystyrene foam particles. FBLWC combined the advantages of normal density concrete, cellular concrete and high workability. FBLWC is currently believed to have a promising future in construction field; as foam balls lightweight concrete has a dry unit weight of 18.50 kN/m³ that leads to self-weight reduction of 15–20%. That results in reducing dead weight, in addition to lower foundation cost with the achievement of a cubic compressive strength of 27 MPa. This paper focuses on investigating and evaluating the short term and the long term behavior of FBLWC. The investigation of the short term behavior focused on studying the compressive strength, splitting tensile strength, modulus of elasticity, stress-strain curve in compression and tension and tension stiffening effect. For the long term behavior, an experimental investigation of FBLWC, in compression and flexure, was performed. The short term behavior and the long term behavior were performed according to the standards of ASTM. Moreover, the results of the investigation are compared to ACI provisions. The experimental results of tested specimens showed that ACI equation's with modification factor $\lambda = 0.75$ for calculating the LWC mechanical properties can be valid for the FBLWC with sufficient accuracy.

Index Terms— Light weight concrete, compressive behavior, creep behavior, splitting tensile strength

1 INTRODUCTION

Lightweight concrete (LWC) has been a feature in the structural construction owing to its advantages over the normal weight concrete (NWC). According to ACI 318R-14, 2014 [3], structural lightweight concrete is defined as a concrete made with lightweight aggregate; the air dried unit weight at 28 days is usually in the range of 14.40 to 19.00 kN/m³ and the cylinder compressive strength is more than 17.2 MPa.

also used.

The mixture consisted of Portland cement, coarse aggregate and sand, in a proportion of 1:1.4:1.4 by weight, 0.3 was the water/cement ratio used for the mix. In addition, 330 liters of foam balls were added to the mix. **Table 1** summarizes the concrete mixes' proportions. The design cube compressive strength "f_{cu}" is 25 MPa.

2 CONSTITUENT MATERIALS AND MIX PROPORTIONING

As a part of ongoing research at the Faculty of Engineering Ain Shams University, an innovative mix design was developed of foam balls lightweight concrete, in which conventional coarse aggregate is partially replaced by polystyrene foam particles. The materials used in this work were gravel, sand, Portland cement, water, foam balls and reinforcement steel bar. In addition to that, superplasticizer and silica fume are

TABLE 1
Concrete mixes' proportions

Component	Weight
Cement	450 Kg
Silica fume	40 kg
Coarse Aggregate	630 kg
Sand	630 kg
Polystyrene Foam balls	330 liters
Super Plasticizer	13.5 liters
Water	139 liters

- *S elkouly is currently Teaching assistant, Construction & Building Department, October 6 University, Cairo, Egypt*
E-mail: s_alkouly.eng@o6u.edu.eg
- *Randa Fouad is currently Teaching assistant, Cairo International College, Cairo, Egypt*
E-mail: randa_fouad@cic-Cairo.com
- *Amr Zaher is currently Professor of concrete structures, Structural Engineering Department, Ain Shams University, Cairo, Egypt.*
E-mail: amr_zaher@eng.asu.edu.eg
- *Ehab F. Sadek is currently Assistant Professor, Structural Engineering Department, Ain Shams University, Cairo, Egypt*
E-mail: hhab.Fawzi@eng.asu.edu.eg
- *Khaled Riad is currently Associate Professor, Structural Engineering Department, Ain Shams University, Cairo, Egypt*
E-mail: khaled_riad@eng.asu.edu.eg

3 EXPERIMENTAL PROGRAM

The experimental program comprised two phases. The first phase was executed to evaluate the short-term behavior of FBLWC, and the second phase was carried out to study the long-term behavior of FBLWC.

TABLE 2
Specifications of the tested specimens

Group No.	Specimens No.	Dimension (mm)	Performed Test	Reinforcement	Density
G1	CU1, CU2, CU3	150X150X150	Compressive strength	-----	18.45 kN/m ³
	CU4, CU5, CU6		Young's Modulus	-----	
	CU7, CU8, CU9		Splitting test	-----	
G2	CY1, CY2, CY3	Diameter 150 Height 300	Compressive strength	-----	
	CY5		Young's Modulus	-----	
	CY4, CY6, CY7, CY8, CY9		Stress-strain curve	-----	
G3	P-12-1, P-12-2, P-12-3	150X150X300	Tension stiffening (Direct tension)	1D12	
	P-16-4, P-16-5, P-16-6			1D16	
	P-18-9			1D18	
G4	S1, S2	Rebar D 12	Tensile strength	-----	
	S3, S4	Rebar D 16		-----	
	S5, S6	Rebar D 18		-----	

3.1 Phase 1: Short-Term Behaviour of FBLWC

Twenty-seven FBLWC specimens of cubes, cylinders and prisms were tested according to the requirements and standards of ASTM C39 [6]. The specimens' properties are given in Table 2.

3.1.1 Compressive Strength Test

Three cubes and three cylindrical specimens were tested to obtain the compressive strength of the FBLWC. The used loading rate was 0.5 N/mm²/sec.

3.1.2 Modulus of Elasticity Test

According to ASTM C 469 [8], a couple of loading and unloading cycles are applied to cylinder specimens with a constant rate of 0.5 N/mm²/sec up to 60 sec. After completing the loading and unloading cycles, the applied stress (σ_b) is kept constant for 60s, and then in the following 30s the average strain (ϵ_b) is recorded. After that, the applied stress is increased with the same rate, mentioned previously; till it reaches (σ_a) and the corresponding average strain (ϵ_a) is measured in the next following 30 seconds. The test set up is shown in Fig. 1. The modulus of elasticity can be determined by the following Eq.(1):

$$E = \Delta\sigma / \Delta\epsilon = (\sigma_a - \sigma_b) / (\epsilon_a - \epsilon_b) \quad (1)$$



Fig. 1. Test setup for E-modulus test

3.1.3 Stress-strain Relationship

The stress-strain relationship was determined for the FBLWC using cubic and cylindrical samples. The test was displacement-controlled, conducted at a minimum rate of 0.5 mm/minute. The specimens were capped by using a poll seating to ensure full contact with the loading head, as shown in Fig 2.



Fig. 2. Test setup of cylindrical specimens for the determination of the stress-strain relationship

3.1.4 Tensile Splitting Strength Test

The tensile strength of FBLWC was measured according to the standard test of ASTM C 496 [9]. This test is referred to as the split cube test. Indirectly it measures the tensile strength of concrete by compressing a cube through a line load applied along its length by using supplementary steel loading plates at a rate of $0.5 \text{ N/mm}^2/\text{s}$, as shown in Fig.3 and Fig. 4.

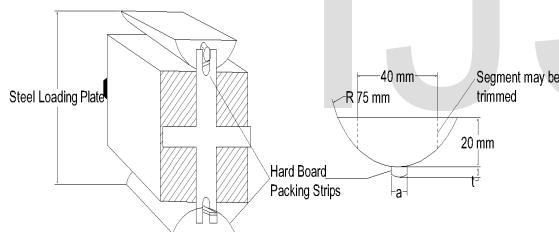


Fig. 3. Cube specimens splitting test setup [9]



Fig. 4. Splitting tensile test on FBLWC specimens

3.1.5 Tension Stiffening

Tension stiffening tests were carried out on prism specimens with dimensions of $150 \times 150 \times 300 \text{ mm}$ with single steel bars of 12, 16 and 18 mm diameter placed in the center of the prism. Specimens were loaded vertically, as shown in Fig.5.



Fig. 5. Test setup for direct tension test

3.2 Phase 2: Long-Term Behavior of FBLWC Tests

This phase is divided into two parts; the first part was executed to cover the determination of the creep of molded FBLWC cylinders subjected to sustained longitudinal compressive load and determination of companion shrinkage for unloaded specimens according to the methods proposed by ASTM C512/C512M [10] and ASTM C157 [7], respectively. The second part was carried out to study time-dependent flexural behavior of FBLWC reinforced beams.

3.2.1 Creep and Shrinkage of FBLWC under Compressive Loading Test

3.2.1.1 Creep Test

- Test Specimens

The test was performed using nine $150 \times 300 \text{ mm}$ FBLWC cylinders and three NWC $150 \times 300 \text{ mm}$ cylinders to compare the creep behavior of both materials. Three load levels were applied: (1) 20% of the ultimate compressive strength of concrete, (2) 40% of the ultimate compressive strength of concrete, and (3) 60% of the ultimate compressive strength of concrete.

- Test Apparatus

The design of the creep test apparatus is shown in Fig.6. Three apparatuses (one for each load level) are manufactured and used in this test. In each test frame, four $150 \times 300 \text{ mm}$ cylindrical specimens (three FBLWC + one NWC) are placed on top of one another and cemented together by epoxy and tested under the same load.

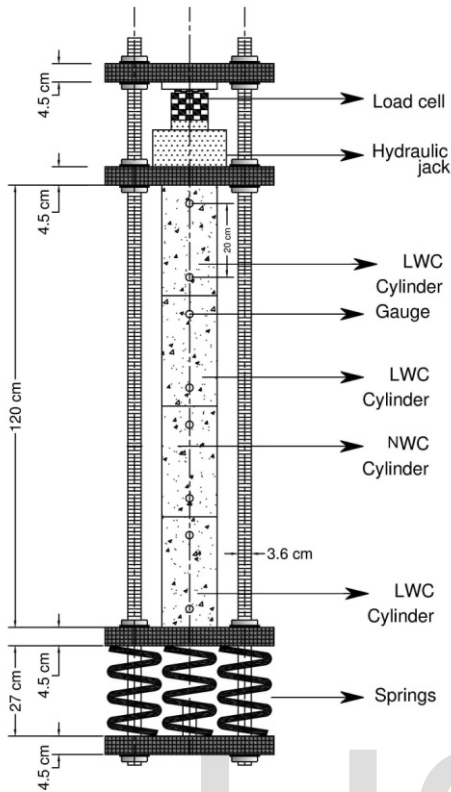


Fig. 6. Design of the creep test apparatus



Fig. 7. The creep test apparatus

- **Test Procedure**

The load is applied using a hydraulic jack and monitored by a load cell with a digital readout indicating the load applied. When the desired load is reached, the nuts on the threaded rods are turned so that they are snugly pressing against the plate underneath the hydraulic jack to hold the plate in that position and thus maintaining the applied load, as shown in Fig.7. Initial readings were taken with the dial gauges after loading. Then measurements were taken every day in the first week, and then once a week till 280 days.

3.2.1.2 Shrinkage Test

The free shrinkage measurements were made using three 75×300 mm concrete prisms specimens for each concrete mixture. Two pairs of gauge studs were placed at both ends of the specimens.

The specimens were removed from the molds at the age of 23 h and then placed in water for a minimum of 30 minutes. At the age of 24 h, the specimens were removed from water storage and wiped with a damp cloth. An initial reading was immediately taken with a length comparator. The specimens were then stored in the drying room and strain measurements on both the loaded (creep) and the unloaded (shrinkage) specimens, are made with the dial gauge at appropriate intervals up to an age of 280 days, and are reported. Fig.8 shows the test set-up of the free shrinkage test.



Fig 8. Free shrinkage test set-up

3.2.2 Time-Dependent Flexural Behavior of Reinforced FBLWC Beams

These tests were performed to evaluate the flexural behavior of reinforced FBLWC beams under sustained load with time, since the creep test in the first part was carried out on unreinforced FBLWC.

3.2.2.1 Test Specimens

Table 3 shows the two groups of beams which were tested under different stress levels. Each group consists of four beams; three beams made of FBLWC mixture and one beam made of NWC mixture to compare its creep behavior with each other. Beams in each of the previous groups subjected to different stress levels had three different percentage of additional compression reinforcement (A_s') to tension reinforcement (A_s). Tension and compression reinforcement steel bars had a yield

stresses equal to 360 N/mm^2 and 240 N/mm^2 , respectively. Fig.9 shows details of the tested beams.

3.2.2.2 Test Apparatus

The same creep test apparatus used in the previous test was used in the flexure test.

3.2.2.3 Instrumentation

The mid-span deflection was measured using dial gauges. In the first two weeks, deflections were recorded daily, and the load was checked. Then, the records were taken every three to four days for a month time; finally, the readings were taken once per week up to an age of 120 days.

3.2.2.4 Test Procedure

The beams in both groups were tested at the age of 28 days. The deflection was noted immediately after applying the full sustained load and was recorded as the immediate deflection. The sustained load was applied for 120 days, and during this period deflection readings were recorded at regular intervals. Fig.10 shows the test setup.



Fig. 10. Point bending creep test

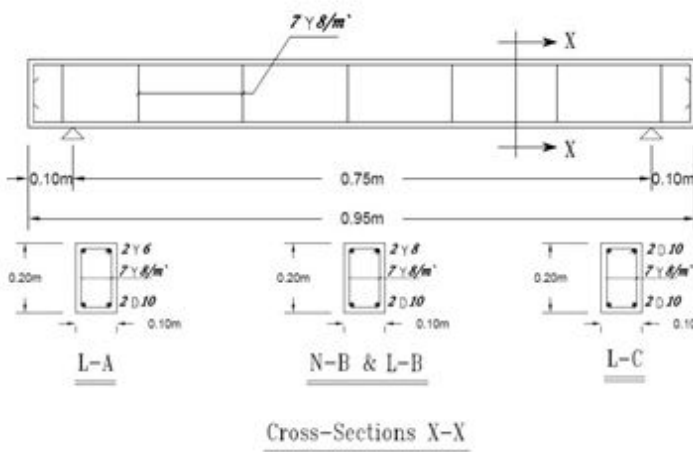


Fig. 9. Concrete dimensions and details of tested beams

TABLE 3
Details of beam specimens

Specimen ID	Stress Level	Concrete Mix	Specimen Dimensions		Tension RFT.	Compression RFT.	As'/As %
			b (mm)	t (mm)			
L-1A	0.25 f_{cu}	FBLWC	100	200	2D10	2Y6	0
L-1B		FBLWC	100	200	2D10	2Y8	60
N-1B		NWC	100	200	2D10	2Y8	60
L-1C		FBLWC	100	200	2D10	2D10	100
L-2A	0.5 f_{cu}	FBLWC	100	200	2D10	2Y6	0
L-2B		FBLWC	100	200	2D10	2Y8	60
N-2B		NWC	100	200	2D10	2Y8	60
L-2C		FBLWC	100	200	2D10	2D10	100

4 EXPERIMENTAL RESULTS AND DISCUSSIONS

This section presents and discusses the results of the various tests conducted on FBLWC specimens in the laboratory for short term and long term behavior.

4.1 Phase 1: Short-Term Behavior Tests Results

4.1.1 Compressive Strength

Generally, the most important mechanical property of concrete is its compressive strength, as all other concrete properties are related to it. For structural LWC, it is aimed to get a reasonable compressive strength accompanied with a significant self-weight reduction. For the tested FBLWC mixture the achieved dry unit weight of 18.45kN/m³, leads to self-weight reduction of about 16%.

Based on Table 4, it can be noticed that the average compressive strength of tested FBLWC cubes and cylinders is 27.0 MPa and 22.4 MPa, respectively. The ratio of the cylinder strength to the cube strength is 0.83.

TABLE 4
Compressive strength results for cube FBLWC

150 mm cube			150x300 mm cylinder		
No	P _f (kN)	f _{cu} (MPa)	No	P _f (kN)	f _{c'} (MPa)
CU1	700	31.1	CY1	360	20.3
CU2	580	25.7	CY2	420	23.7
CU3	530	23.5	CY3	410	23.2
Average	610	27.0	Average	390	22.4

– Failure Pattern of Specimens

The failure cracks of cube specimens are approximately parallel to the direction of load, as shown in Fig. 11 with some cracks formed at an angle to the applied load. As a result, lateral shearing stress is produced in the cube specimen. The effect of this shear decrease towards the center of cubes; so these sides of the cube have near vertical cracks at the cube center.



Fig. 11. Failure pattern of cube specimen (CU1)

4.1.2 Static Modulus of Elasticity

The results of the static modulus for elasticity test are shown in Fig. 12. The elasticity modulus of concrete is considered as the slope between the calculated stresses vs. the calculated strains. From the experimental results, the obtained average modulus of elasticity is 17385 MPa.

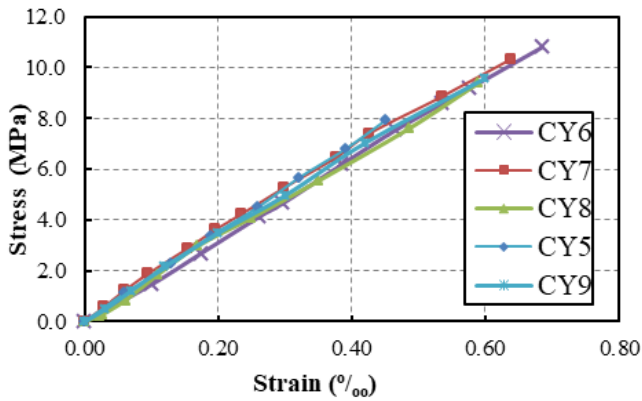


Fig. 12. Stress-strain curve measured during E-modulus Test (3rd loading cycle)

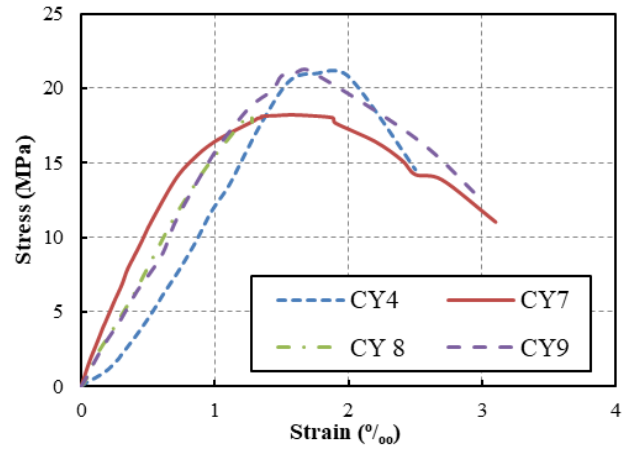


Fig. 13. The stress-strain curve for all specimens

The modulus of the elasticity of concrete may be precisely expressed as a function of the compressive strength of concrete. It is the way that most codes are using to calculate the modulus of elasticity of concrete. For instance, the ACI [3] expresses the Young's modulus as in EQ. (2).

$$E_c = 0.043W_c^{1.5} (f_c')^{0.5} \quad (2)$$

Where W_c (the concrete unit weight in kg/m^3) is $1845 \text{ kg}/\text{m}^3$ and f_c' (cylinder compressive strength in MPa) is 22.40 MPa , the modulus of elasticity from Eq. (2) is 16128 MPa . That shows good agreement between static modulus of elasticity obtained experimentally and that obtained from EQ. (2) (Difference = 7.2%).

The ratio between Young's modulus of LWC and NWC having the same compressive strength is about $\frac{1}{4}$ to $\frac{1}{5}$ as suggested in [4, 10, 12]. By using EQ. (2), the modulus of elasticity for NWC (unit weight is $2200 \text{ kg}/\text{m}^3$) having same concrete strength is 21000 MPa . The ratio between the experimental modulus of elasticity of FBLWC and modulus of elasticity of NWC from EQ (2) is 0.828, which is higher than the suggested values.

4.1.3 Stress-Strain Curves

The behavior of concrete is a strain-softening behavior, indicating a reduction in stress after the peak value with an increase in the deformation. Although the ductility of concrete is much lower than steel, it still exhibits significant deformation before fracture. Fig. 13 shows the stress-strain curve for CY4, CY7, CY8 and CY9 cylinder specimens.

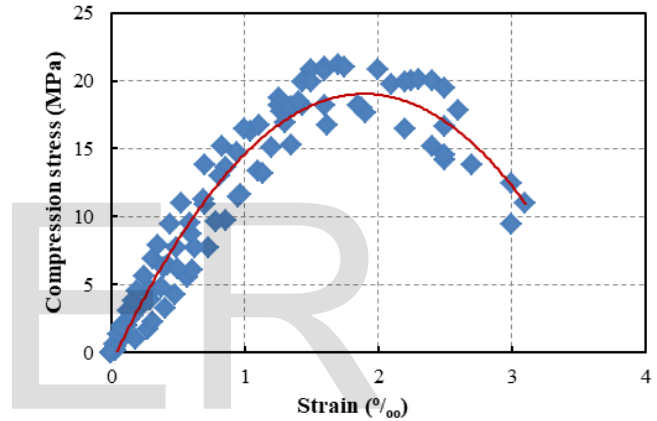


Fig. 14. Average stress-strain curve of all specimens

From Fig. 15, the obtained design stress-strain curve, has a linear elastic behavior up to $(40\% f_c')$. The softening curve up to the crushing of concrete is at $(63\% f_c')$. The maximum crushing strain ϵ_u is $3.00 (o/oo)$, and the strain at the ultimate strength of concrete ϵ_0 is $1.90 (o/oo)$. The stress strain relation after the linear part can be expressed by Eq. (3).

$$f_c = - 0.27x f_c' (\epsilon_c)^2 + f_c' (\epsilon_c) \quad (3)$$

Where:

f_c' : FBLWC cylinder compressive stress in MPa

f_c : FBLWC stress in MPa

ϵ_c : strain (o/oo)

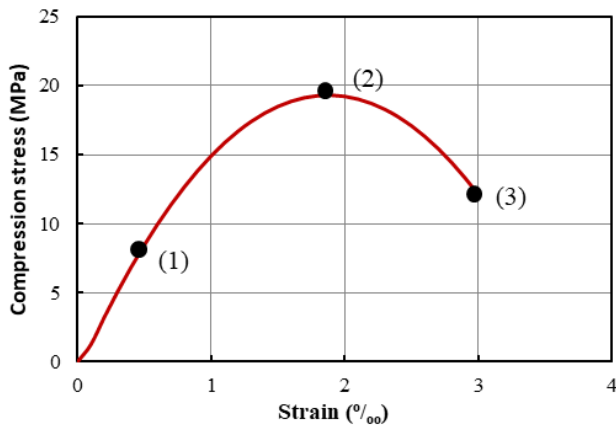


Fig. 15. The obtained design stress-strain curve for FBLWC

4.1.4 Tensile Splitting Strength and Modulus of Rupture

The structural properties of normal weight and lightweight concrete, such as the shear resistance, bond strength and the resistance to cracking, depend on the tensile strength. The higher the tensile strength is, the better the structural properties will be. Table 5 gives splitting tensile strength of three 150x150x150 mm FBLWC cube specimens.

TABLE 5

values of the splitting tensile strength of the FBLWC cubes

Spec.	Applied load (kN)	Splitting tensile strength (MPa)	Average splitting strength (MPa)	Compressive strength (MPa)
CU7	73.8	2.08	1.81	C22.4/27.0
CU8	62.7	1.77		
CU9	56.1	1.58		

According to the ACI [3] the splitting tensile strength for lightweight concrete is calculated by using a modification factor " λ " as a multiplier for the equation $0.56*(f_c')^{0.5}$ used for NWC, where $\lambda = 0.75$ for all-lightweight concrete types. The calculated splitting tensile strength for tested FBLWC is 1.90 MPa. The ratio between splitting tensile strength obtained experimentally (1.81 MPa) and the calculated value for tested FBLWC is about 95%. Hence, the equation mentioned above can be used for the determination of FBLWC tensile splitting strength.

4.1.5 Tension stiffening of lightweight foamed concrete

4.1.5.1 Failure Pattern of Specimens

For tested FBLWC prisms, one can first observe the appearance of the initial transverse crack near the center of prism length. Then, under a higher load, the splitting cracks phenomenon appeared and the concrete body was segmented into separate blocks for deformations at near yielding of the reinforcing. Longitudinal splitting cracks could be detected at the end of specimen elements. This occurred for large deformations, usually beyond yielding of the steel reinforcing bar. This might be explained by the Poisson's effect and the high splitting pressure due to the deformation of the reinforcing bar. At last, a secondary transverse network of cracks had grown from the splitting crack. The cracking pattern evolved when the steel failed, as shown in Fig. 16.



Fig. 16. Lateral cracks due to direct tension test for FBLWC

4.1.5.2 Test results of embedded bars in FBLWC prisms

Fig. 17, Fig. 18 and Fig. 19 show the tensile stress-strain curves for rebars embedded in FBLWC prisms, and subjected to direct tension. The corresponding curve of a bare rebar tested is also plotted. The figures are the average of three tested specimens of each steel bar diameter. The difference between the two curves represents the contribution of the surrounding concrete in tension. The stress-strain curve for reinforced concrete under uniaxial tension can be divided in three regions: pre cracking, crack development and post cracking region.

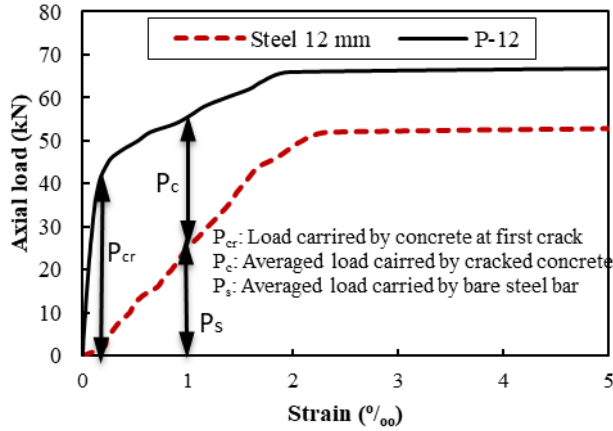


Fig. 17. Tensile stress-strain relationships for (P-D12)

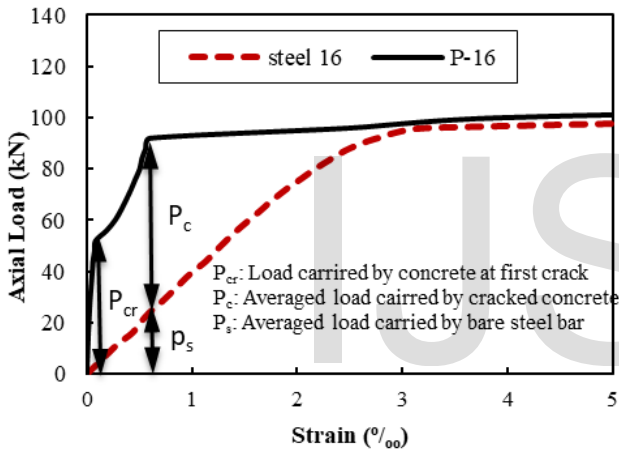


Fig. 18. Tensile stress-strain relationships for (P-16)

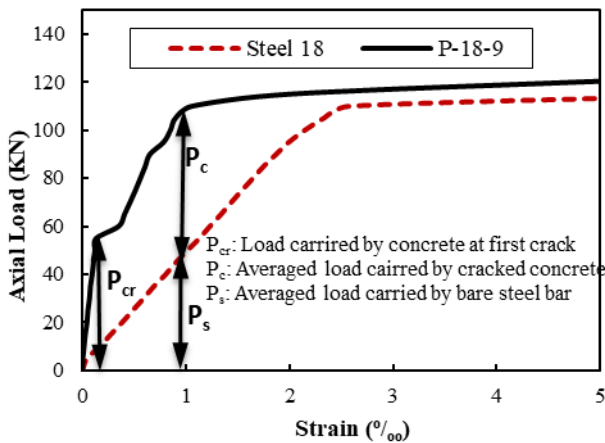


Fig. 19. Tensile stress-strain relationships (P-18-9)

4.1.5.3 Determination of Actual Tensile Stress-Strain Curve of FBLWC

The stress-strain relationship of FBLWC in tension contains two parts. The first part is the ascending part. It is clear that the tensile stress of concrete increases linearly with increasing strain up to first crack. The second one is the descending part. After cracking, the tensile stress decreases monotonically with increasing strain up to failure.

- **Part 1: For the ascending part of tensile stress-strain curve "Tension-Stiffening":**

The prism is initially assumed to be uncracked and under a uniform strain corresponding to a total axial force P_T causing a stress f_t in the concrete and f_s in the steel, as shown in Eq. (4).

$$P_T = f_t \cdot A_c + f_s \cdot A_s \quad (4)$$

The cracking stress f_{cr} is determined by computing the stress using the experimentally obtained cracking load, as given in Eq. (5). Table 6 is showing the obtained tensile stresses and the corresponding strains for the tested specimens.

$$f_{cr} = P_{cr} / (A_c + n \cdot A_s) \quad (5)$$

TABLE 6
The stress and the strain at first crack

Sample No.	Cracking load P_{cr} (kN)	Stress (MPa)	Strain (‰)
P-12	38	1.59	0.12
P-16	52	2.09	0.12
P-18	54	2.12	0.13

- **Part 2: For the descending part of the tensile stress-strain curve "Tension-softening":**

A tensile stress-strain curve has been evaluated in this study based on the load shared between steel bars and surrounded by foam balls lightweight concrete. The shaded area between the two curves in Fig. 20 represents the concrete contribution in the pre-cracking and the post-cracking ranges.

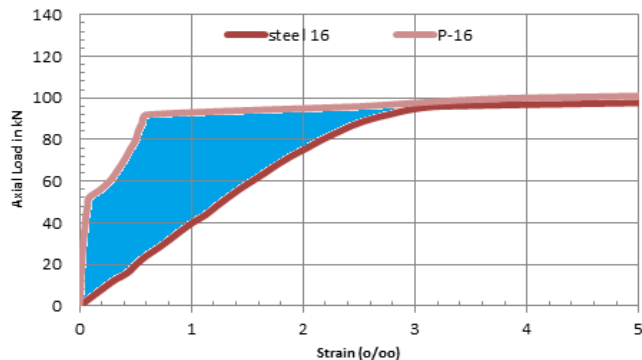


Fig. 20. Tensile stress-strain relationships for bare and embedded bar

Tension stress is calculated by determining P_c , P_{sr} and P_{cr} . The descending parts of P-12, P-16 and P-18 specimens, which are shown in Fig. 21, are plotted by the given equation (6).

$$f_t = P_c / (A_c + n \cdot A_s) \tag{6}$$

Where:

- f_{cr} Average stresses at first crack;
- f_t Average stresses at the cracked member;
- P_{cr} Average loads at first crack;
- A_c Concrete area of the member;
- A_s Area of steel;
- n The modular ratio of elasticity = E_s/E_c
= 200000/17385 and is equal to 11.50;
- E_c Young's modulus of concrete;
- E_s Young's modulus of steel.

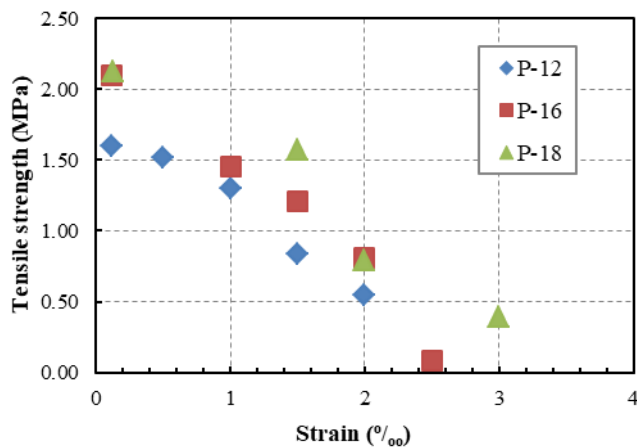


Fig. 21. The descending part for the tested specimens

The proposed stress-strain curve in Fig. 22 is the average of P-12, P-16 and P-18. The curve assumes a linear relationship up to the concrete cracking strength f_{cr} . The tensile strength of tested FBLWC is about (7-8) % of its cube compressive strength, as shown in Fig. 23.

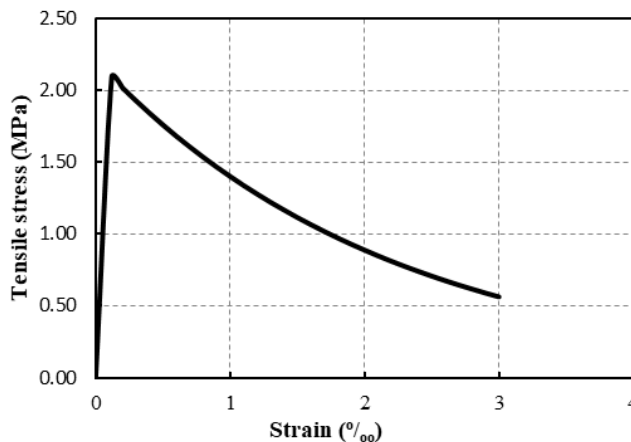


Fig. 22. Tensile stress-strain relationship of FBLWC

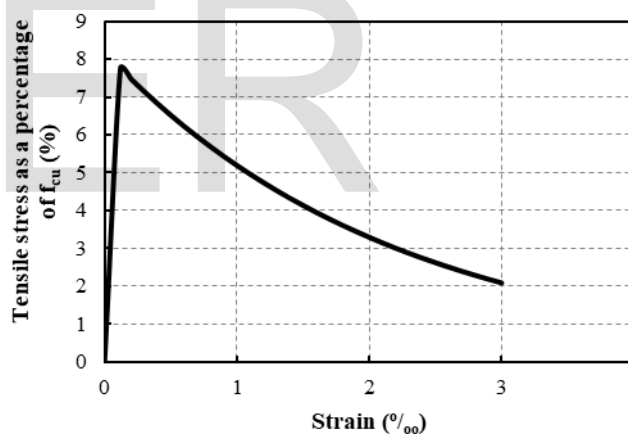


Fig. 23. Tensile stress-strain relationship of FBLWC as a percentage of compressive strength

After cracking, where the average strain ϵ_c exceeds the cracking strain ϵ_{cr} , the proposed stress-strain curve can be calculated, as the given in the following Eq. (7).

$$f_t = 0.13 \epsilon_c^2 - 0.9 \epsilon_c + f_{cr} \tag{7}$$

Where:

- f_{cr} Average stresses at first crack;
- f_t Average stresses at the cracked member;
- ϵ_c Strain (o/oo)

4.2 Phase 2: Long-Term Behavior Tests Results

4.2.1 Creep and Shrinkage of FBLWC under Compressive Loading Test Results

4.2.1.1 Comparison between FBLWC and NWC mixtures

• Shrinkage Test Results

The tested FBLWC had relatively higher shrinkage than NWC with increasing percentage of 31%, as shown in Fig. 24. Although FBLWC recorded higher shrinkage strains than NWC, these shrinkage strains were considerably low than those concluded from previous study [12]. This was attributed to using a lower water/cement ratio in FBLWC mixture than the ratio in the NWC mixture. FBLWC shrinkage strain was 0.0399% at the end of the test.

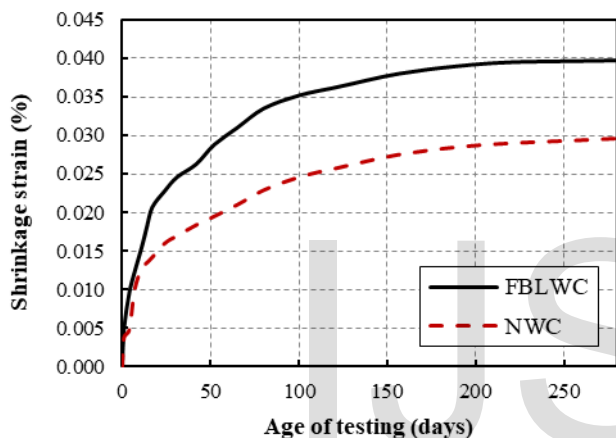


Fig. 24. Shrinkage strains of the two concrete mixtures evaluated

• Creep Test Results

- Creep Strain

The creep strain was calculated by subtracting the shrinkage strain and the elastic strain from the total measured strain. From Figs. 25 to 27, it can be noticed that the creep strains of FBLWC were equal to or lower than the creep strains of the NWC, in spite of the fact that concretes made of lightweight aggregates are expected to exhibit higher creep than those made with hard aggregates. Generally, the strength of the FBLWC is lower than the strength of NWC of the same w/c ratio and, to obtain the same strength, the former concrete must be prepared with a lower w/c ratio than the latter one. Thus, w/c ratio in FBLWC mix was 0.308 while in NWC mix was 0.4. The lower w/c ratio reduces the creep of the cement paste of FBLWC, and this reduction counteracts the increased creep, which is brought about by the use of the lightweight aggregates.

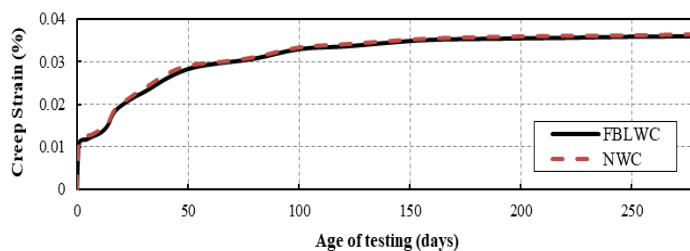


Fig. 25. Creep Strain of FBLWC and NWC (20% load level)

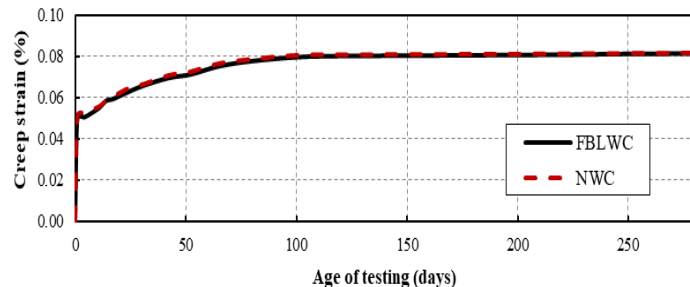


Fig. 26. Creep Strain of FBLWC and NWC (40% load level)

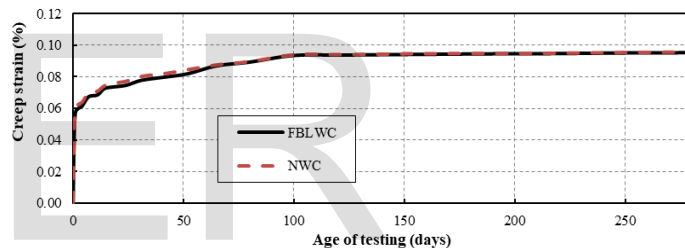


Fig. 27. Creep Strain of FBLWC and NWC (60% load level)

ACI 209.2R-08 [4] was used to estimate strains due to creep in tested concrete specimens. The estimated strains, using the measured values for the elastic modulus of the concrete and compressive strength determined from phase 1, are compared to measured creep strains from phase 2. For each stress level, creep strains were calculated at ages 3, 7, 14, 31, 65, 100, 190 and 280 days and are compared to measured creep strain values at same ages as shown in Fig.28. The used model predicts the FBLWC creep strains with sufficient accuracy.

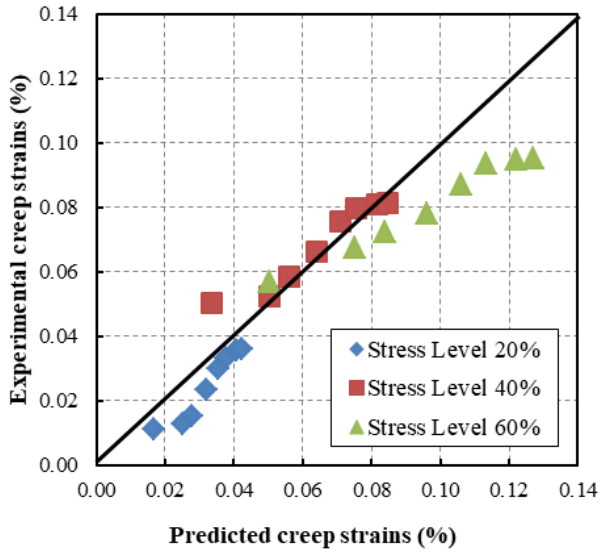


Fig. 28. Creep strains prediction of the ACI model compared to measured values

- Creep Coefficient

The Creep coefficient (ϕ), as defined in ACI-318R-14 [3], is a ratio of creep strain to elastic strain, and is a dimensionless quantity. The creep coefficient was calculated by dividing the creep strain by the elastic strain. Fig.29 shows that the creep coefficients of FBLWC are substantially lower than those of NWC and this is because of the massive difference of the two concrete mixtures elastic strains. Creep coefficient of FBLWC is about 36% lower than creep coefficient of NWC.

It also can be observed that the three different stress levels had nearly no effect on the creep coefficient of FBLWC mix.

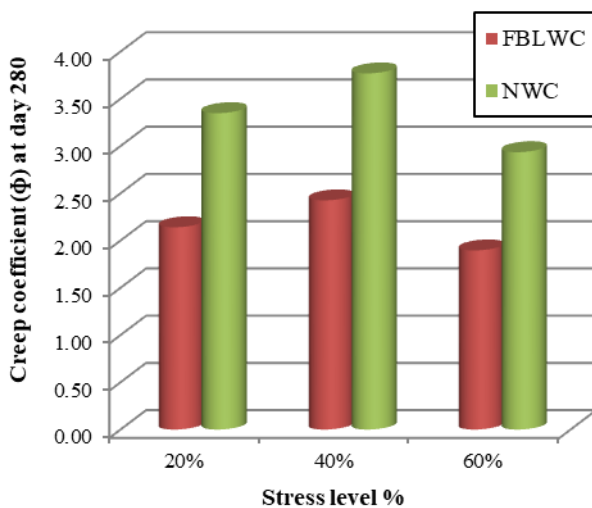


Fig. 29. Creep Coefficient of FBLWC and NWC after 280 days of sustained load

• Time-Dependent Strain

The time-dependent strain (shrinkage plus creep) of FBLWC specimens were higher than those of NWC specimens with about 9%.

Fig.30 shows the measured time dependent strains (shrinkage plus creep) of FBLWC and NWC after 280 days of sustained load. The magnitudes of the elastic strain, shrinkage plus creep strain, shrinkage strain, creep strain, and total strain of the FBLWC at 280 days are summarized in Table 7.

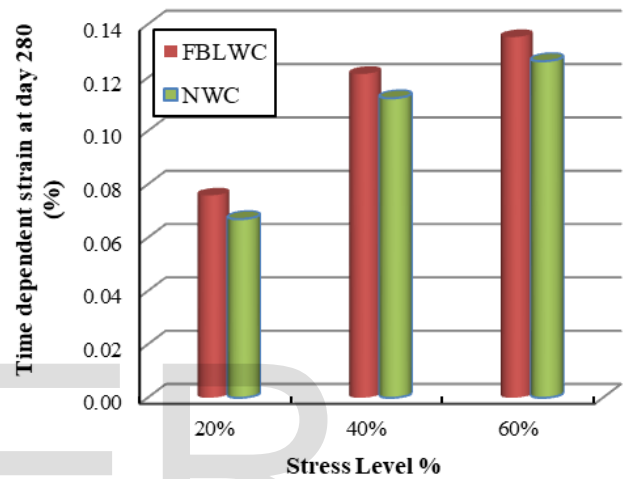


Fig. 30. Time dependent strain of FBLWC and NWC after 280 days of sustained load

TABLE 7
RELATIVE MAGNITUDES OF STRAINS AFTER 280 DAYS OF SUSTAINED LOAD

Load Level	Mixture Type	Elastic Strain (%)		Shrinkage + creep (%)		Shrinkage (%)		Creep (%)		Total Strain (%)	
		mm/mm	(%)	mm/mm	(%)	mm/mm	(%)	mm/mm	(%)	mm/mm	(%)
20%	FBLWC	0.0168	154	0.0759	113	0.0399	131	0.0360	99	0.0927	119
	NWC	0.0109	100	0.0670	100	0.0300	100	0.0365	100	0.0779	100
40%	FBLWC	0.0336	154	0.1214	108	0.0399	131	0.0815	100	0.155	116
	NWC	0.0217	100	0.1123	100	0.0300	100	0.0818	100	0.134	100
60%	FBLWC	0.0503	154	0.1353	107	0.0399	131	0.0954	100	0.1856	117
	NWC	0.0451	100	0.1262	100	0.0300	100	0.0957	100	0.1588	100

4.2.1.2 Effect of Stress to Strength Ratio on Creep Strain

Fig.31 shows a linear relation between creep strain and stress to strength ratio up to a ratio of 0.6. The following simple linear function was used to develop the relationship:

$$\epsilon_{c280} = \alpha \left(\frac{\text{Stress}}{\text{Strength}} \text{ ratio} \right) + \beta$$

$$= 0.0015 (\text{stress/strength ratio}) + 0.001$$

where ϵ_{c280} is the creep strain at 280 days. Using this relationship, the creep strain of FBLWC under different stress levels can be approximated by knowing the concrete strength.

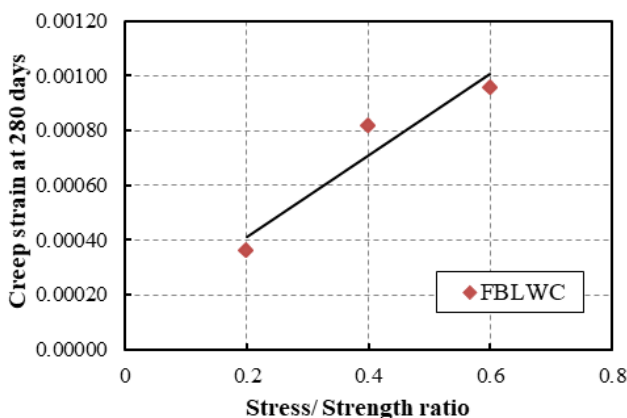


Fig. 31. Relation between stress level and creep strain at 280 days for FBLWC specimen

4.2.2 Time-Dependent Flexural Behavior of Reinforced FBLWC Beams Test Results

Table 8 gives the measured immediate deflection (Δ_i), time-dependent deflection at 120 days- the end of loading time- ($\Delta_{120} - \Delta_i$), and the ratio between them (λ).

TABLE 8
IMMEDIATE DEFLECTION, TIME-DEPENDENT DEFLECTION, AND TIME-DEPENDENT DEFLECTION RATIO FOR FBLWC BEAMS

Beam name	stress level	(Δ_i) (mm)	($\Delta_{120} - \Delta_i$) (mm)	$\lambda = (\Delta_{120} - \Delta_i) / \Delta_i$
L-1A	25%	0.125	0.059	0.472
L-1B	25%	0.117	0.045	0.385
L-1C	25%	0.113	0.042	0.372
L-2A	50%	0.362	0.115	0.318
L-2B	50%	0.337	0.095	0.282
L-2C	50%	0.318	0.085	0.267

It can be noticed from previous table, a linear relationship between the immediate deflection (Δ_i) and time-dependent deflection ($\Delta_{120} - \Delta_i$) at day 120, end of loading period.

4.2.2.1 Comparison between FBLWC and NWC Beams
FBLWC beams had higher time-dependent deflection than that of NWC beams by 23% as shown in Fig. 32. This may be attributed to the higher restrained shrinkage strains of FBLWC causing higher long-term deflections.

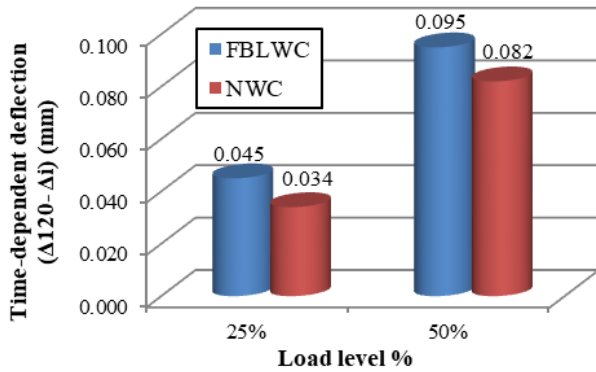


Fig. 32. Time dependent deflections of LWC and NWC beams after 120 days of sustained load

For each reinforced FBLWC beam, in the two groups, time-dependent deflections were calculated by ACI 209R-92 model [4] at age of 120 day and compared to measured time-dependent deflection values at same age as shown in Fig.33. To some extent, the ACI model gives a good prediction of time-dependent deflections of FBLWC and this because of the multiplier factor (λ) in ACI model depends on the additional steel reinforcement and time of applying the sustained load on the concrete element.

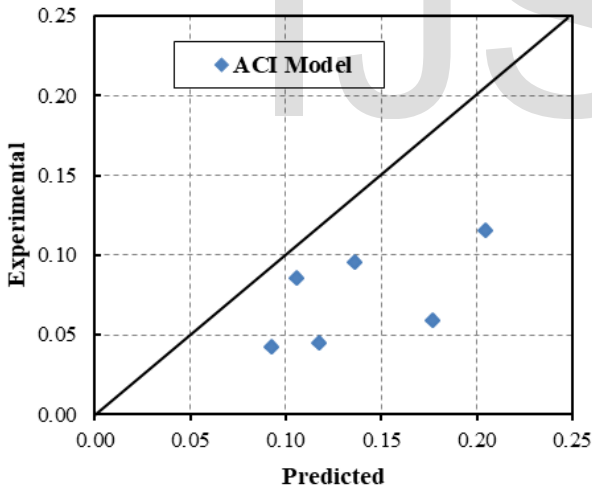


Fig. 33. Time-dependent deflections predicted from ACI compared to measured time-dependent deflections

4.2.2.2 Effect of A_s'/A_s Ratio on The Time-Dependent Deflection

It can be observed from Figs.34 and 35 that the compression steel has the effect of significantly reducing the time-dependent deflections. The addition of compression reinforcement reduced the long-term deflections, almost after one week since loading, and the beneficial effect of compression reinforcement in reducing long-term deflections increased with increase in the ratio A_s'/A_s .

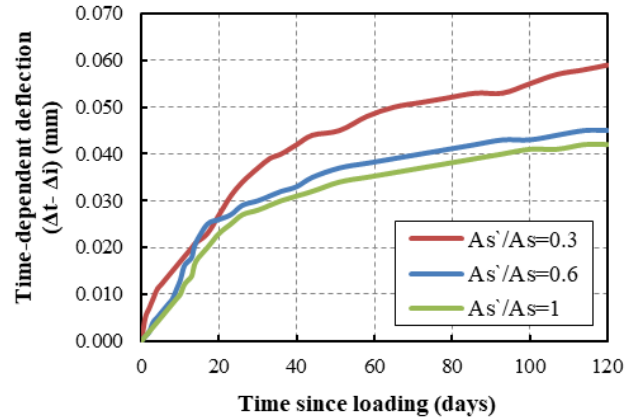


Fig. 34. Time-dependent deflections for different additional compression reinforcement, load-level 25%

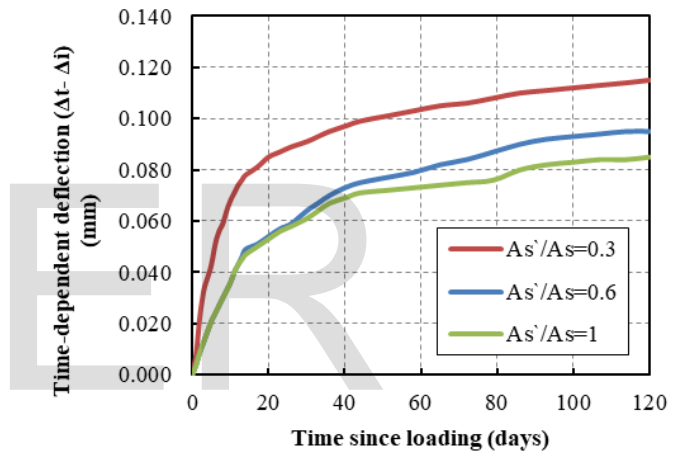


Fig. 35. Time-dependent deflections for different additional compression reinforcement, load-level 50%

However, little improvement in the effectiveness of compression reinforcement in controlling the time-dependent deflection ratio (λ) was noted when A_s'/A_s was increased to 1.

4.2.2.3 Effect of Load Level on The Time-Dependent Deflection

Time-dependent deflection ($\Delta_{120} - \Delta_i$) has been affected by the applied load level as shown in Fig.36. It can be noticed that the relation between the load level and the time-dependent deflection is linear which is almost agreed with the same conclusion stated before in 4.2.1.2.

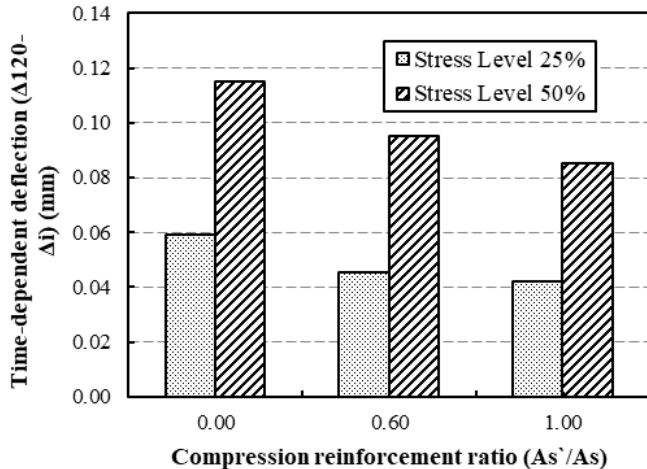


Fig. 36. Time-dependent deflection at day 120 for different applied load level

5 CONCLUSION

For the tested FBLWC specimens, it can be concluded that:

- 1) A uniaxial stress-strain curve was developed for FBLWC with C22.4/27 MPa considering the post peak behavior in compression and tension.
- 2) ACI equation's with modification factor ($\lambda = 0.75$) for calculating the FBLWC mechanical properties can be used for the developed FBLWC with sufficient accuracy.
- 3) The tested FBLWC has a significantly higher drying shrinkage than the NWC with 31%.
- 4) The creep strain of tested FBLWC is equal to that of NWC during the test period, and this may be attributed to the lower w/c ratio used for the FBLWC mix producing a denser paste with less porosity.
- 5) The time-dependent strain (shrinkage plus creep) of the tested FBLWC is significantly higher than that of NWC with 9%.
- 6) The creep strains of FBLWC are proportional to the applied stress to strength ratio.
- 7) The time-dependent deflections of the FBLWC beams are higher than those of NWC beams with of 23%. This may be attributed to the higher restrained shrinkage strains of FBLWC causing higher long-term deflections.

6 REFERENCES

- [1] A. Farghal Maree and K. Hilal Riad, (2014), "Analytical and experimental investigation for bond behaviour of newly developed polystyrene foam particles' lightweight concrete", *Engineering Structures* 58 (2014) 1-11.
- [2] A. Neville and J. Brooks, "Concrete Technology", Prentice-Hall, 2010.

- [3] ACI Committee 318, 2014, *Building Code Requirements for Structural Concrete (ACI 318-14) and Commentary (ACI 318R-14)*, American Concrete Institute, Farmington Hills, MI, 430 pp.
- [4] ACI COMMITTEE 209R-92 (Reapproved 1997), *Prediction of Creep, Shrinkage and Temperature Effects in Concrete Structures, Part 1*, ACI Manual of Concrete Practice 2007.
- [5] Akinkulore, O.O., (2014), "A Comparative Analysis Of Modulus Of Rupture And Splitting Tensile Strength Of Recycled Aggregate Concrete", *American Journal Of Engineering Research (AJER)* E-ISSN: 2320-0847 P-ISSN: 2320-0936 Volume-03, Issue-02, Pp-141-147.
- [6] ASTM C 39. (2012), "Standard Test Method for Compressive Strength of Cylindrical Concrete Specimens", *Annual Book of Standards Volume 04.02*, ASTM International, West Conshohocken, PA.
- [7] ASTM Standard C157, "Standard Test Method for Length Change of Hardened Hydraulic-Cement Mortar and Concrete".
- [8] ASTM C 469. (2012), "Standard Test Method for Static Modulus of Elasticity and Poisson's Ratio of Concrete in Compression", ASTM International, West Conshohocken, PA.
- [9] ASTM C 496 "Standard Test Method for Splitting Tensile Strength of Cylindrical Concrete Specimens"
- [10] ASTM C512/C512M, "Standard Test Method for Creep of Concrete in Compression".
- [11] Funso. F., Efe. I. & Christopher. F., (2013), "A Study On The Compressive And Tensile Strength Of Foamed Concrete Containing Pulverized Bone As A Partial Replacement Of Cement", *Pak. J. Engg. & Appl. Sci.* Vol. 13, July, 2013 (P. 82-93).
- [12] Sabaa, B., Ravindrarajah, R. S., "Engineering Properties Concrete Containing Crushed Expanded Polystyrene Waste", Faculty of Engineering, University of Technology, Sydney, Australia, 1997